Journal of Sound and Vibration (2000) **238**(4), 617–635
doi:10.1006/jsvi.2000.3089, available online at http://www.idealibrary.com on IDEAL®

CRACK IDENTIFICATION USING HYBRID NEURO-GENETIC TECHNIQUE

M.-W. SUH AND M.-B. SHIM

School of Mechanical Engineering, Sung kyun kwan University, Jangan-Gu, Suwon Kyoungki-Do, 440-746, *South Korea. E-mail: suhmw@yurim.skku.ac.kr*

AND

M.-Y. KIM

School of Civil Engineering, Sung kyun kwan University, Jangan-Gu, Suwon Kyoungki-Do, 440-746, *South Korea*

(*Received* 6 *July* 1999, *and in final form* 4 *May* 2000)

It has been established that a crack has an important effect on the dynamic behavior of a structure. This effect depends mainly on the location and depth of the crack. To identify the location and depth of a crack on a structure, a method is presented in this paper which uses hybrid neuro-genetic technique. Feed-forward multi-layer neural networks trained by back-propagation are used to learn the input (the location and depth of a crack)–output (the structural eigenfrequencies) relation of the structural system. With this trained neural network, genetic algorithm is used to identify the crack location and depth minimizing the difference from the measured frequencies.

1. INTRODUCTION

Techniques to detect cracks and defects hidden in a structure and to evaluate their residual life time are very important to assure the structural integrity of operating plants and structures. Many researchers have investigated the potential of system identification to determine the properties of a structure. A state of damage could be detected by a reduction in stiffness. A crack, which occurs in a structural element, causes some local variations in its stiffness which affects the dynamics of the whole structure to a considerable degree. An analysis of the changes is tried to identify the crack. Most of the studies on crack identification problem have adopted the modal parameter or the dynamic response to identify the global stiffness and mass matrices of a structure.

A crack in a structure introduces a local flexibility, which is a function of the crack depth. This flexibility changes the stiffness and the dynamic behavior of the structure. Chondros and Dimarogonas [1, 2] considered the crack as a local elasticity, which effects the elasticity of the whole cracked structure under consideration and related the crack depth with the frequency decrease. Gounaris and Dimarogonas [3] have constructed a special cracked beam finite element and Papadopoulos and Dimarogonas [4] used a 6×6 compliance matrix, including off-diagonal terms, to simulate a cracked shaft and to study its dynamic behavior.

A number of papers deal with the problem of crack location and size identification in order to propose new, efficient and more precise methods. Inagaki *et al.* [5] used a procedure with eigenfrequency measurements to find the crack size and location. Leung

0022-460X/00/490617 + 19 $35.00/0

[6] and Anifantis *et al.* [7] proposed crack identification methods through the measurements of the dynamic behavior in bending. Dimarogonas and Massouros [8] investigated the dynamic behavior of a circumferentially cracked shaft in torsion and proposed nomographs for finding the crack depth and the location. Nikolakopoulos *et al.* [9] presented the dependency of the structural eigenfrequencies on crack depth and location in contour graph form. To identify the location and depth of a crack, they determined the intersection points of the superposed contours that correspond to the measured eigenfrequency variations caused by the presence of the crack. However, the intersecting points of the superposed contours are not only difficult to find but also incorrect to evaluate since the procedure mainly depends on the physical eye.

The use of neural networks in detecting the damage has been developed for several years, because of their ability to cope with the analysis of the structural damage without the necessity for intensive computation. Recently, neural networks are expected to be a necessity for intensive computation. Recently, neural networks are expected to be a potential approach to detect the damage of the structure [10–14]. In these researches, both the modal frequencies and the modal shapes are needed for the training of neural network to detect the structural damage, since the frequency information alone is not sufficient to train the neural network for the inverse problem of the crack identification.

To identify the location and depth of a crack in a structure with only frequency information, a method is presented in this paper which uses hybrid neuro-genetic technique. Feed-forward multi-layer neural networks trained by back-propagation are used to learn the input (the location and depth of a crack)–output (the structural eigenfrequencies) relation of the structural system. With this trained neural network, genetic algorithm is used to identify the crack location and depth minimizing the difference from the measured frequencies. Our approach needs only the modal frequencies for we use hybrid neuro-genetic techniques.

2. INVERSE ANALYSIS METHOD

The inverse analysis is generally defined as identifying the parameter set $x^* \in X$ when measured, or reference data $y^* \in Y$ and direct mapping $\psi : X \to Y$ are known. Problems with the non-linear direct mapping ψ are termed non-linear inverse problems. In practice, deterministic models describe reality only in an idealized sense, and thus we may express the input–output relation as follows:

$$y = \psi(\mathrm{x}) + \varepsilon, \tag{1}$$

where $\varepsilon = \varepsilon_1 + \varepsilon_2$, and ε_1 and ε_2 are the errors in the measurement of y and those in the model equations respectively.

In the analysis of field quantities shown in Figure 1, the model equations in general take the form

$$L(k)\phi = q, \tag{2}$$

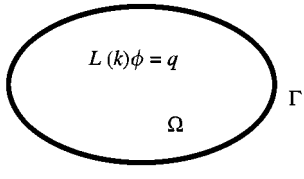

Figure 1. Problems of field quantities: Ω: domain; Γ: boundary.

where L, k, ϕ, q are the differential operator, material property, field quantity and a source term respectively.

Inverse problems for equation (2) can be classified in terms of the parameter set to be identified: (a) domain Ω, (b) governing equations, (c) boundary conditions, (d) force or source q applying in Ω, (e) material properties k defined in Ω and involved in the governing equations [10, 11]. In these problems, the input and output vectors reside in the continuous space. There are two main strategies for solving inverse problems. One is to solve a set of equations and the other is to directly find the minimum or maximum of a certain function. However, the former is worth noting the following difficulty: the inverse problem can always be defined as an abstract theoretical concept. In general, inverse function is a subset of original input, in fact such a subset could even be empty, so that the usual concept of "function" as a "one-to-one" injection breaks down. Generally, it is reasonable to solve the latter. Out of them, minimizing a least-squares criterion has been most widely used for identification.

In this approach, optimization techniques are used to find the input by adjusting them until the measured, or reference data match the corresponding data computed from the parameter set in the least-squares fashion, i.e.,

$$\min f(x) \tag{3a}$$

with the cost functional

$$f(x) = \sum_{i=1}^{m} k_i (y_i^* - \Psi_i(x))^2, \tag{3b}$$

where k_i is a weighting factor. Various calculus-based optimization techniques have been intensively used to solve this optimization problem. These techniques can, however, fail if errors contained in the model equations and in the measurement cause the objective function to be complex. In such cases, the solution may result in a local minimum, unless some regularization method is incorporated. The present study uses genetic algorithm, which is significantly promising for complex optimization.

3. STRUCTURE ANALYSIS

In the finite element model of the damaged structure, the effect of the crack on the behavior of the structure can be simulated through the introduction of the transfer matrices which are methods for finding the stiffness matrix. A planar frame structure can be modelled using two-dimensional beam elements having three degrees of freedom (d.o.f.) (δ_x, δ_y, θ_z) per node, that is, with extension and bending, as in Figure 2.

The corresponding stiffness and consistent mass local matrices [15] are

$$[K_e] = \frac{EI_{zz}}{L^3} \begin{bmatrix} \beta L^2 & 0 & 0 & -\beta L^2 & 0 & 0 \\ 0 & 12 & 6L & 0 & -12 & 6L \\ 0 & 6L & 4L^2 & 0 & -6L & 2L^2 \\ -\beta L^2 & 0 & 0 & \beta L^2 & 0 & 0 \\ 0 & -12 & -6L & 0 & 12 & -6L \\ 0 & 6L & 2L^2 & 0 & -6L & 4L^2 \end{bmatrix}, \tag{4}$$

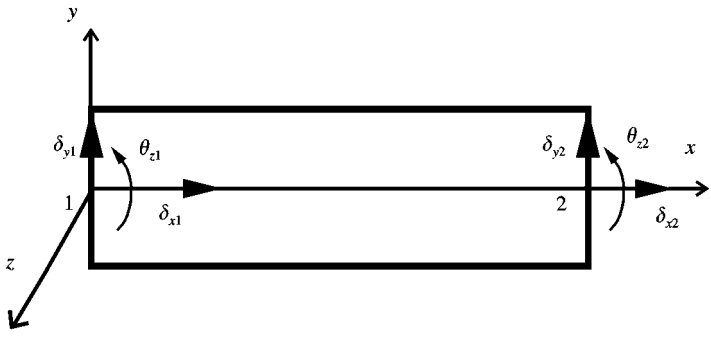

Figure 2. A beam finite element with extension and bending.

$$[M_e] = \frac{\rho AL}{420}\begin{bmatrix} 140 & 0 & 0 & 70 & 0 & 0 \\ 0 & 156 & 22L & 0 & 54 & -13L \\ 0 & 22L & 4L^2 & 0 & 13L & -3L^2 \\ 70 & 0 & 0 & 140 & 0 & 0 \\ 0 & 54 & 13L & 0 & 156 & -22L \\ 0 & -13L & -3L^2 & 0 & -22L & 4L^2 \end{bmatrix}, \tag{5}$$

where $\beta = A/I_{zz}$, L is the length of element e, and A is the cross-sectional area. E and ρ are the modulus of elasticity and mass density, respectively, and I_{zz} is the second moment of inertia about the local z-axis.

From the Euler–Bernoulli theory for the above-mentioned d.o.f., the transfer matrix [15] which transfers the state variables (displacement, force) from one node to the other node, is

$$[T_e] = \begin{bmatrix} 1 & 0 & 0 & \dfrac{-L}{AE} & 0 & 0 \\ 0 & 1 & L & 0 & \dfrac{L^3}{6EL_{zz}} & -\dfrac{L^2}{6EI_{zz}} \\ 0 & 0 & 1 & 0 & \dfrac{L^2}{2EI_{zz}} & \dfrac{L}{EI_{zz}} \\ 0 & 0 & 0 & -1 & 0 & 0 \\ 0 & 0 & 0 & 0 & -1 & 0 \\ 0 & 0 & 0 & 0 & L & -1 \end{bmatrix}. \tag{6}$$

A beam finite element of length L_e, containing a crack of depth α at distance L_{1e} from its left end, is depicted in Figure 3.

The crack introduces a local compliance in the structure. The state vectors at positions i, C_L, C_R, and j are

$$\{z_i\} = \{\delta_{xi}\ \delta_{yi}\ \theta_{zi}\ F_{xi}\ F_{yi}\ M_{zi}\}^{\mathrm{T}}, \qquad \{z_L\} = \{\delta_{xL}\ \delta_{yL}\ \theta_{zL}\ F_{xL}\ F_{yL}\ M_{zL}\}^{\mathrm{T}}, \tag{7a, b}$$

$$\{z_R\} = \{\delta_{xR}\ \delta_{yR}\ \theta_{zR}\ F_{xR}\ F_{yR}\ M_{zR}\}^{\mathrm{T}}, \ \{z_j\} = \{\delta_{xj}\ \delta_{yj}\ \theta_{zj}\ F_{xj}\ F_{yj}\ M_{zj}\}^{\mathrm{T}}. \tag{7c, d}$$

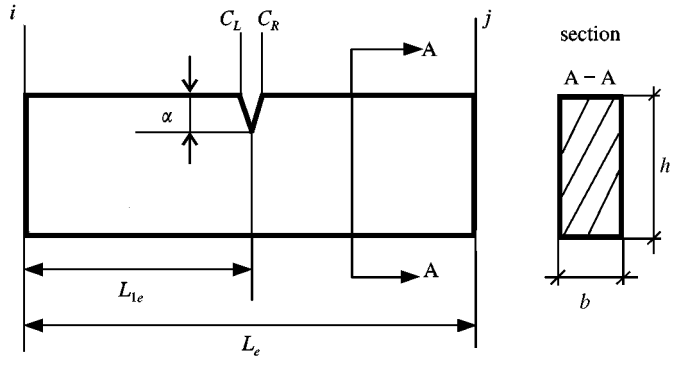

Figure 3. A cracked beam finite element.

If no force is acting between nodes i and j, then it can be derive from simple beam theory, where the four state vectors are related as follows:

$$\{z_L\} = [T_1]\{z_i\}, \qquad \{z_R\} = [T_C]\{z_L\}, \qquad \{z_j\} = [T_2]\{z_R\}, \tag{8a–c}$$

where $[T_1]$ and $[T_2]$ are the transfer matrices of the subelements $C_L - i$ and $C_R - j$, respectively, and $[T_C]$ is the point transfer matrix due to the crack. Matrix $[T_C]$, which relates the state vectors on the left and right of the crack, is

$$[T_C] = \begin{bmatrix} 1 & 0 & 0 & c_{11} & 0 & c_{13} \\ 0 & 1 & L & 0 & c_{22} & 0 \\ 0 & 0 & 1 & c_{31} & 0 & c_{33} \\ 0 & 0 & 0 & -1 & 0 & 0 \\ 0 & 0 & 0 & 0 & -1 & 0 \\ 0 & 0 & 0 & 0 & 0 & -1 \end{bmatrix}, \tag{9}$$

where subscripts 1, 2 and 3 correspond to tension, shear and bending respectively. Terms c_{13} and c_{31}, responsible for the coupling of tension and bending [3], are not considered here, whereas the rest are known to be as follows [16]:

$$c_{11} = \frac{2\Phi_1}{E(1-\nu^2)b}, \qquad c_{22} = \frac{2k^2\Phi_3}{E(1-\nu^2)b}, \qquad c_{33} = \frac{72\Phi_2}{E(1-\nu^2)bh^2}, \tag{10a–c}$$

where ν is the Poisson ratio, k is a constant which for rectangular cross-sections is known to be 1·5 and Φ_i are functions of the non-dimensional crack depth α/h [16]. These functions, which are presented in Figure 4, are integrals of the empirical formulas used by Tada [17] for the computation of stress intensity factors K_1 in single-edge notch specimens under pure tension, bending and shear.

From equations (8a–c) the following is obtained:

$$\{z_j\} = [T_e^C]\{z_i\}. \tag{11}$$

The transfer matrix $[T_e^C]$ of the cracked element is written in the form

$$[T_e^C] = [T_2][T_C][T_1] = \begin{bmatrix} A_1 & A_2 \\ A_3 & A_4 \end{bmatrix}, \tag{12}$$

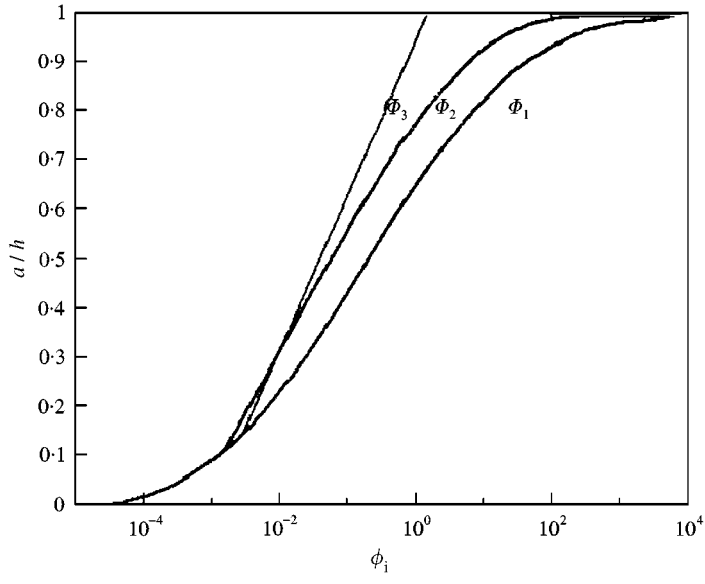

Figure 4. Φ_i versus α/h for single-edge notch specimen under pure tension, bending and shear.

where $[A_i]$ are 3×3 submatrices. Equation (12) leads to the stiffness matrix of the crack element

$$[K_e^C] = \begin{bmatrix} -[A^2]^{-1}[A_1] & [A_2]^{-1} \\ [A_3] - [A_4][A_2]^{-1}[A_1] & [A_4][A_2]^{-1} \end{bmatrix}. \tag{13}$$

The equation of motion in matrix form is known to be

$$(-\omega^2[M] + [K])\{x\} = \{0\}, \tag{14}$$

where ω is the eigenfrequency, and x the displacement vector. The above analysis serves to identify the location and depth of a crack in a frame structure, just by measuring the eigenfrequency variations.

4. NEURAL NETWORK AND GENETIC ALGORITHM

The cracked structure in this study is discretized into a set of elements and the crack is assumed to be located within one of the elements. A neural network for the cracked structure is trained to approximate the response of the structure by the data set prepared through the finite element analysis for various crack sizes and locations. For estimating the location and size of a crack genetic algorithm is utilized, based on the trained neural network. The neural network and the genetic algorithm are utilized for the so-called on-line and the off-line function. The off-line performance is training the input–output pairs including the location and depth of a crack as input and the structural eigenfrequencies as output. The on-line performance is maximizing the fitness function evaluations of all individuals in each generation. Neural network and genetic algorithm will be introduced in the following sections, focused on our application.

4.1. NEURAL NETWORK

Studies on neural networks have been motivated to imitate the way that the brain operates. A network is described in terms of the individual neurons, the network connectivity, the weights associated with various interconnections between neurons, and the activation function for each neuron. The network maps an input vector from one space to another. The mapping is not specified, but is learned. The network is presented with a given set of inputs and their associated outputs. The learning process is used to determine proper interconnection weights and the network is trained to make proper associations between the inputs and their corresponding outputs. Once trained, the network provides rapid mapping of a given input into the desired output quantities. This, in turn, can be used to enhance the efficiency of the design process.

Consider a single neuron. This neuron receives a set of n inputs, x_i, $i = 1, \ldots, n$, from its neighboring neurons and a bias whose value is equal to one. Each of the inputs has a weight (gain) w_{ji} connecting between the ith and the jth units. The weighted sum of the inputs determines the activity of a neuron, and is given as

$$net_j = \sum_{j=1}^{n} w_{ji} x_i. \tag{15}$$

A simple function is now used to provide a mapping from the n-dimensional space of the inputs into a one-dimensional space which comprises of an output value a neuron sends to its neighbors. The output of a neuron is a function of its activity:

$$y = f(net). \tag{16}$$

Many types of neural networks have been proposed by changing the network topology, node characteristics, and the learning procedures. In this study, we use the back-propagation network, that is, a multi-layer feed-forward neural network topology with one hidden-layer as shown in Figure 5. A back-propagation network consists of an input layer, hidden layers, an output layer and adaptive connections between successive layers. Back-propagation networks can be learned when presented with input-target output pairs.

The back-propagation is used usually for its "supervised" learning. It is essentially a special purpose steepest descent algorithm to adjust the w_{ji} connection strengths, and other additional internal parameters that are sometimes added to increase flexibility, to

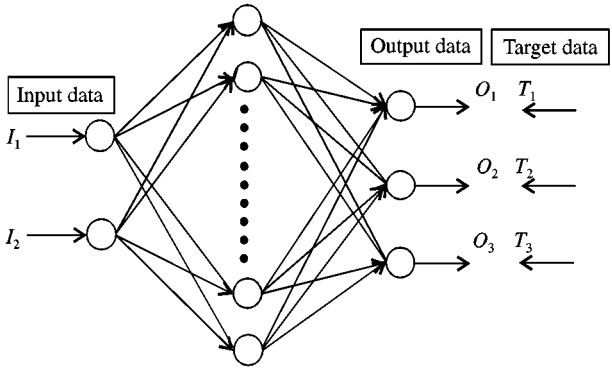

Figure 5. Three-layer neural network utilized in this study.

reproduce the output of given input–output training sets within a required error tolerance. The following training error is defined:

$$E = \sum_{p=1}^{n} E_p = \sum_{p=1}^{n} \sum_{k=1}^{m} (T_{pk} - O_{pk})^2, \tag{17}$$

where E_p is the square error for the pth training pattern, T_{pk} is the teacher signal to the kth unit in the output layer for the pth training pattern, O_{pk} is the output signal from the kth unit in the output layer for the pth training pattern, and m is the number of output units and n is the number of patterns respectively. In the training process, the connection weights w_{ji} is modified repeatedly based on the steepest descent method in order to minimize the above square error:

$$\Delta w_{ji} = -\eta \frac{\partial E}{\partial w_{ji}}, \qquad w_{ji}^{new} = w_{ji}^{old} + \Delta w_{ji}, \tag{18}$$

where η is the learning rate constant. The training is sensitive to the choices of the various net learning parameters. The first parameter is the "learning rate" which essentially groverns the "step size", a concept familiar to the optimization community, and the learning rate constant should be updated according to the following rule:

$$\Delta\eta = \begin{cases} +a & \text{if } \Delta E > 0 \text{ consistently,} \\ -b\eta & \text{if } \Delta E < 0, \\ 0 & \text{otherwise.} \end{cases} \tag{19}$$

This learning rate approach is an adaptive learning constant. The second parameter is the "momentum coefficient" which forces the search to continue in the same direction so as to aid the numerical stability, and furthermore, to go over local minima encountered in the search. This scheme is implemented by giving a contribution from the previous time step to each weight change:

$$\Delta w(n) = -\eta \nabla E(n) + \alpha \Delta w(n-1), \tag{20}$$

where $\alpha \in [0, 1]$ is a momentum parameter and a value as 0·9 is often used. The momentum term typically helps to speed up the convergence and to achieve an efficient and more reliable learning profile.

4.2. GENETIC ALGORITHM

Genetic algorithm is probabilistic optimization algorithm based on the model of natural evolution and the algorithm has clearly demonstrated its capability to create good approximate solutions in complex optimization problems. Figure 6 shows the fundamental structure of the genetic algorithm.

First, a population of individuals, each represented by a vector, is initially generated at random. The population then evolves towards better regions of the search space by means of randomized processes of recombination, mutation and selection. In the recombination, parental individuals breed offspring's individuals by combining part of information from parental individuals. The mutation forms new individuals by making large alterations with small possibility to the offspring individuals regardless of their inheritant information. With the evaluation of fitness for all the individuals, the selection favorably selects individuals of higher fitness to produce more often than those of lower fitness. These reproduction forms

```
t = 0;
Initialize P(t);
do
        Crossover P(t);
        Mutate P(t);
        Evaluate P(t);
        select P(t);
        t = t +1;
While terminal condition is not satisfied
```

Figure 6. Fundamental structure of the genetic algorithm.

one generation of the evolutionary process, which corresponds to one iteration in the algorithm, and the iteration is repeated until a given terminal criterion is satisfied.

5. HYBRID NEURO-GENTIC TECHNIQUE FOR CRACK IDENTIFICATION

For the crack identification, it is known that the crack parameters such as the location and depth of a crack can be determined from the measured eigenfrequencies of structure. This can be classified as the inverse problem. In this study, hybrid neuro-genetic technique is adopted to identify the crack parameters in a structure.

Overall procedure of this study is shown in Figure 7. There is preparation phase and application phase. In the preparation phase, firstly, the learning data of various sets of crack parameters and the corresponding response of the structure, which is the eigenfrequency in this study, are prepared by the computational structure analysis which is presented in section 3. The neural network described in section 4 is adopted to approximate the response of the cracked structure from the prepared learning data.

In the application phase the parameters which identify the crack are estimated by the genetic algorithm described in section 4 using the trained neural network for the fitness function evaluation.

5.1. NEURAL NETWORK TRAINING

The clamped–free beam of Figure 8 has a length of $L = 3$ m, rectangular cross-section $B \times H = 0{\cdot}2 \times 0{\cdot}2$ m and contains a crack of depth α at a distance L_1 from the clamped end. The material properties are $E = 2{\cdot}07 \times 10^{11}$ N/m^2, $\nu = 0{\cdot}3$, and $\rho = 7700$ kg m^3. The beam is discretized into 12 two-node finite elements. For the preparation of the learning data, 10 sets of a crack depth $\alpha = 0{\cdot}01, 0{\cdot}02, \ldots, 0{\cdot}1$ m (step size $= 0{\cdot}01$ m) are introduced at the 29 different locations $L_1 = 0{\cdot}1, 0{\cdot}2, \ldots, 2{\cdot}9$ m (step size $= 0{\cdot}1$ m). Totally 290 cases or patterns (10 different crack depths and 29 different crack locations) are solved for the first three eigenfrequencies. The patterns which consist of 290 sets of data are used to train the neural network of Figure 9.

Because of the nature of the sigmoid activation function, i.e., saturation function, the output variables should be scaled by the user, to be within the most active range of the sigmoid function. Scaling rule that minimum and maximum values are set to 0·1 and 0·9 is

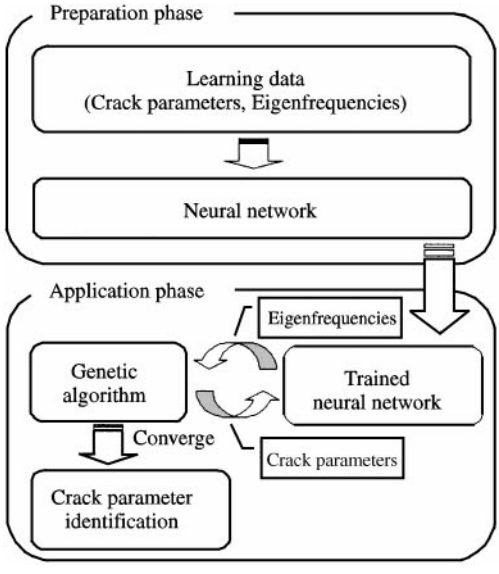

Figure 7. Crack identification procedure on hybrid-neuro-genetic algorithm.

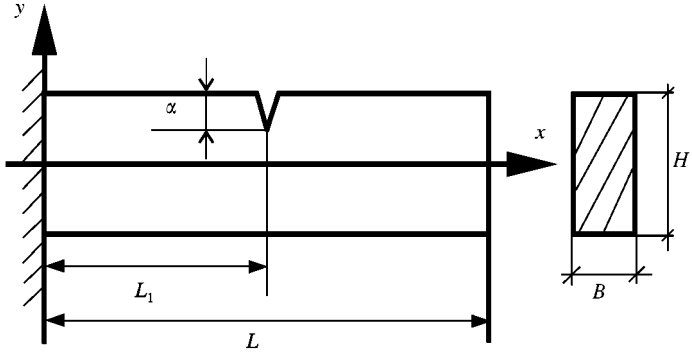

Figure 8. Model of the cracked clamped–free beam.

usually suggested. Through some trials, a network with neuron arrangement (input–hidden–output) of 2–13–3 trained with 100 000 iteration for the 290 patterns are concluded to be the best for our application. In addition, to attain the stable convergence in the training process the momentum coefficient of equation (18) is set to 0·9 and to speed up the convergence the adaptive learning rate of equation (20) is used. That is, if the error decreases the learning rate is increased by 1·05. Otherwise, the learning rate is decreased by 0·7.

Mean-square error (MSE) is employed as a measurement of modelling performance. The mathematical expression can be described as follows:

$$MSE = \frac{\sum_{i=1}^{N} (e_i)^2}{N}, \tag{21}$$

where e_i denotes an error at pattern i and N is the total number of patterns. As shown in Figure 10 the final MSE is 0·0027.

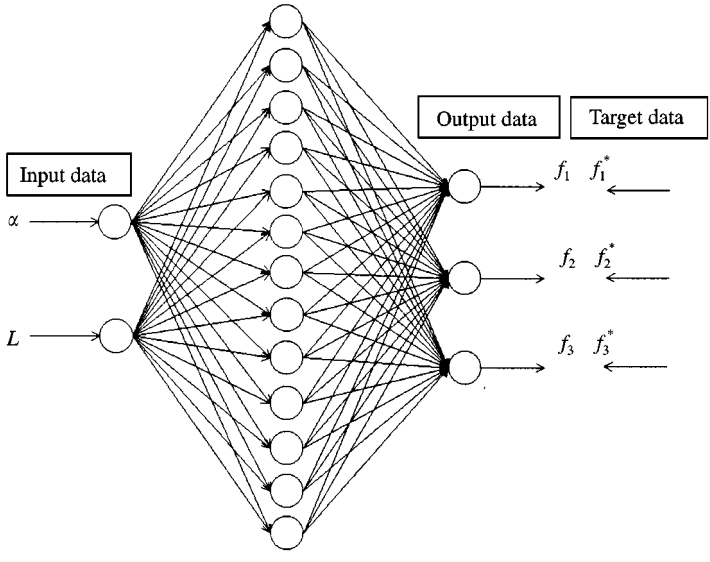

Figure 9. Three-layer neural network with neuron arrangement of 2–13–3.

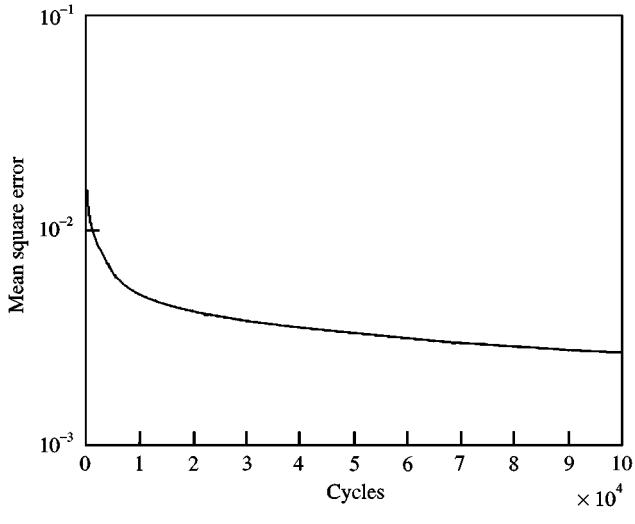

Figure 10. Neural network training output.

The estimated eigenfrequencies from the network are compared to the target values as shown in Figure 11. The target values are f_1^*, f_2^* and f_3^* in Figure 9 which are the reference data or training data to have trained the neural network. Two hundred and ninty patterns are arranged in 10 separate curves base on the value of α as shown in the Figure. The first eigenfrequency f_1 is monotonously increasing as the crack location moves from the clamped end to the free end when the crack depth α is kept constant. On the other hand, the second and the third eigenfrequencies oscillate under the same situation.

It is notable that it can be challenged to estimate the crack depth and the location from the measured eigenfrequencies directly from a new neural network whose input and output data are eigenfrequencies and the crack parameters respectively. This neural network can be

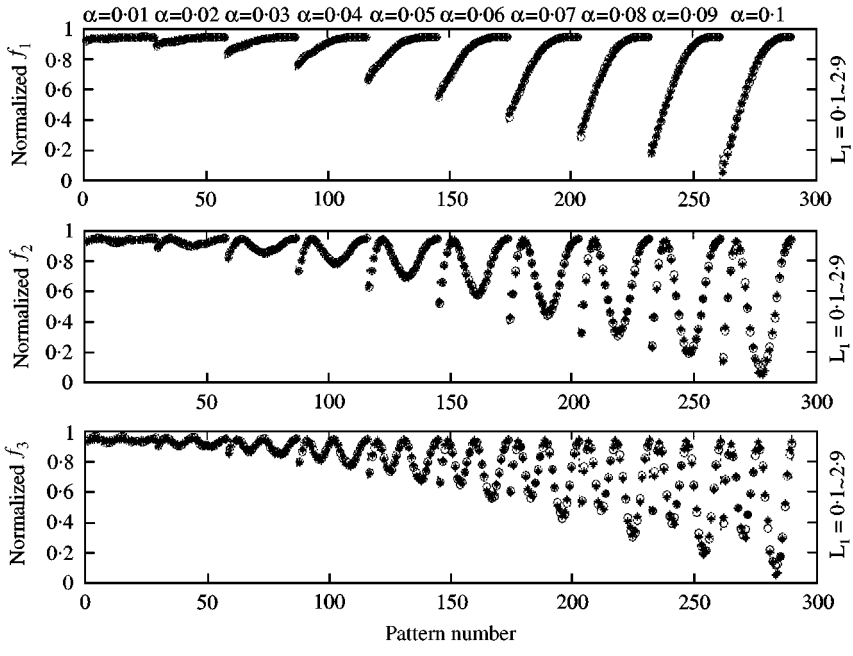

Figure 11. Comparison of the estimated eigenfrequencies from the neural network to target values: ∗ target value; ○ estimated value.

trained with the same patterns, which is used for the network of Figure 9. The difference is that the input data are eigenfrequencies and the target data are crack parameters, α and L_1 for the new neural network. If the new neural network works the crack parameter can be directly obtained from the measured frequencies. Unfortunately, however, the new neural network has been confirmed not to give proper solution. This is due to the fact that the crack parameters cannot be one-to-one functions of the eigenfrequencies. This is the reason why the damage detection researches [10–14] needed the modal shape information in addition to the frequency information.

This is the basis for the optimization work utilizing genetic algorithm which will be introduced in the next section which is necessary for the detection with frequency information above.

5.2. CRACK IDENTIFICATION USING HYBRID NEURO-GENETIC TECHNIQUE

Using the results of the previous section, one can construct crack identification problem in terms of optimization with genetic algorithm. The fitness function for the genetic algorithm to be maximized is defined as follows:

$$\max_{a,l_1} F = \frac{1}{a + \sum_{i=1}^{3} (f_i - f_i^*)^2}, \qquad 0{\cdot}01 \leqslant \alpha \leqslant 0{\cdot}1, \quad 0{\cdot}1 \leqslant L_1 \leqslant 2{\cdot}9, \tag{22}$$

where α is the depth of a crack, L_1 is the distance from the clamped end, a is a constant used to build a well-defined fitness function, f_1, f_2, f_3 are the first three eigenfrequencies which are

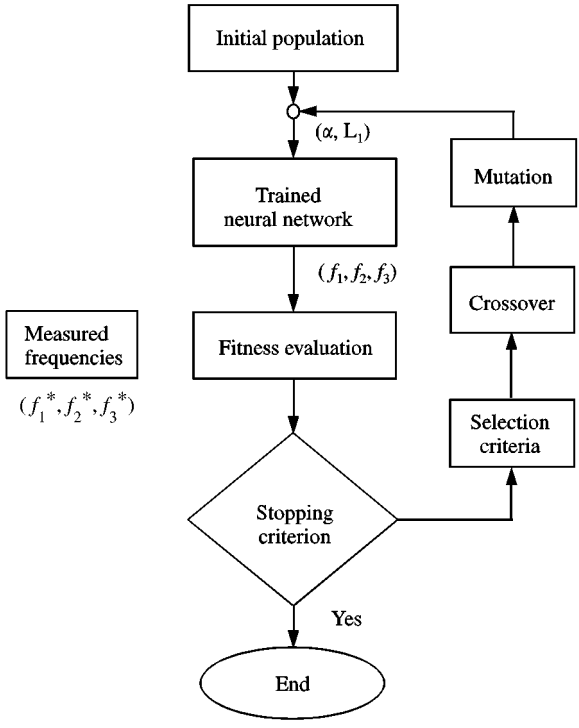

Figure 12. Flowchart of the hybrid neuro-genetic technique.

functions of α and L_1; and f_1^*, f_2^*, f_3^* are the first three measured, or reference eigenfrequencies.

The general procedure is illustrated in Figure 12. The previously trained neural network is utilized for the calculation of the first three frequencies as the functions of the crack depth (α) and distance (L_1). Through several test problems, the genetic algorithm for this study is set-up: population size, $N = 100$; crossover rate, $C = 0{\cdot}25$; mutation rate, $M = 0{\cdot}01$. Also, each parameter is represented as a 25-bit binary number, roulette wheel selection method is adopted for the selection.

5.3. EXAMPLE PROBLEM 1: CLAMPED–FREE BEAM

A cracked clamped–free beam of Figure 8 is adopted as an example problem, two cases are considered. (a) A crack of depth α of 0·02 m exists at L_1 of 0·3 m. The first three eigenfrequencies are obtained computationally based on the theory described in section 3: $f_1^* = 113{\cdot}48$ rad/s, $f_2^* = 714{\cdot}46$ rad/s, $f_3^* = 2007{\cdot}56$ rad/s. (b) A crack of depth α of 0·06 m exists at L_1 of 0·1 m. The first three eigenfrequencies are obtained computationally; $f_1^* = 110{\cdot}34$ rad/s, $f_2^* = 702{\cdot}09$ rad/s, $f_3^* = 1910{\cdot}37$ rad/s.

The hybrid neuro-genetic technique has been applied to this example problem. Figures 13 and 14 illustrate convergence history of the fitness function for case (a) and case (b) respectively. The searches meet the convergence after 84 and 47 iterations for case (a) and case (b) respectively. The result of Table 1 shows that the location and depth of a crack are estimated by the hybrid neuro-genetic technique within 5% error. Also, the corresponding eigenfrequencies are very close to the reference values within 0·15% error.

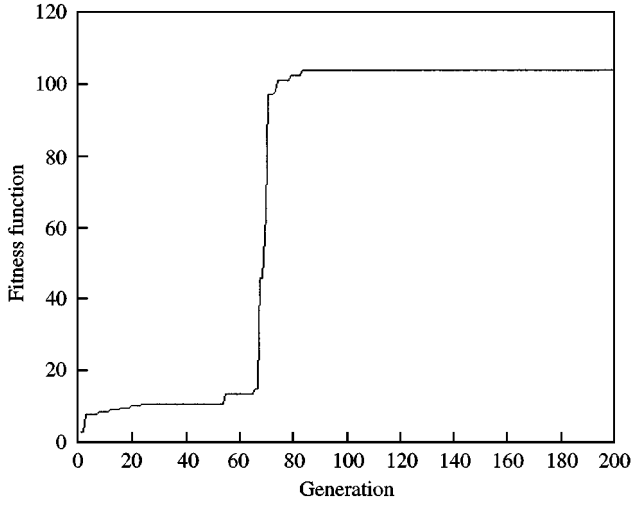

Figure 13. Generation history of Case (a).

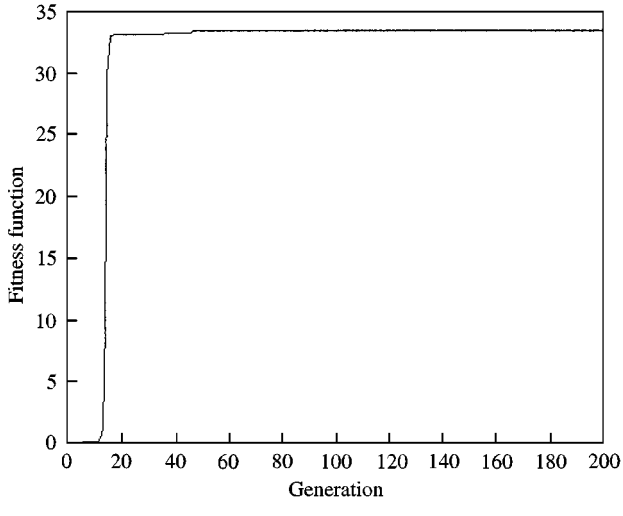

Figure 14. Generation history of Case (b).

5.4. EXAMPLE PROBLEM 2: CLAMPED—CLAMPED PLANE FRAME

A crack in the clamped–clamped plane frame, shown in Figure 15 is identified using the methodology of this study. The frame has the following basic dimensions; $b \times h = 0{\cdot}15\ \text{m} \times 0{\cdot}2\ \text{m}$ and $B \times H = 0{\cdot}008\ \text{m} \times 0{\cdot}016\ \text{m}$. The frame is discretized into 24 two-node finite elements. Since there is a vertical axis of symmetry, the crack location for the half of the frame is considered. For the preparation of the learning data, nine sets of a crack of depth $\alpha = 0{\cdot}0016,\ 0{\cdot}0024, \ldots, 0{\cdot}008\ \text{m}$ (step size $= 0{\cdot}0008\ \text{m}$) are introduced at the 11 different locations $L_1 = 0{\cdot}4125,\ 0{\cdot}6875, \ldots, 3{\cdot}1625\ \text{m}$ (step size $= 0{\cdot}275\ \text{m}$). Totally 99 cases or patterns are solved for the first three eigenfrequencies. These patterns are used to train the

TABLE 1

Crack identification result: *clamped–free beam*

	Case (a)			Case (b)		
	Reference value	Result value	Relative error (%)	Reference value	Result value	Relative error (%)
a (m)	0·02	0·021	5	0·06	0·061	1·6
L_1 (m)	0·3	0·310	3	1·0	0·997	− 0·3
f_1 (rad/s)	113·48	113·38	− 0·08	110·34	110·17	− 0·15
f_2 (rad/s)	714·46	714·44	− 0·003	702·09	701·88	− 0·03
f_3 (rad/s)	2007·56	2007·61	0·002	1910·37	1910·40	0·001

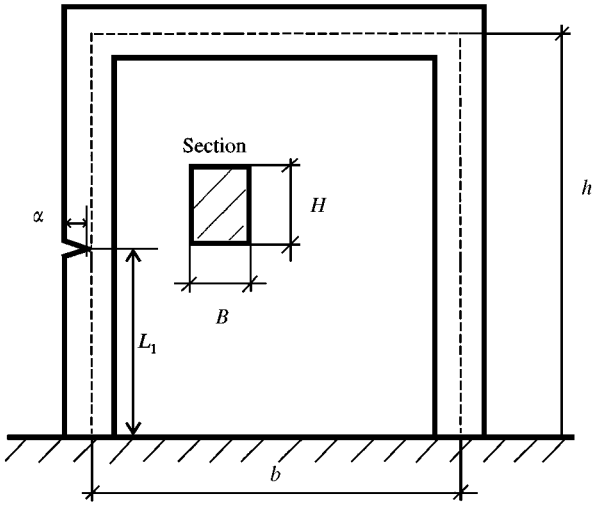

Figure 15. Clamped–clamped plane frame.

neural network of Figure 9. Figure 16 shows the training accuracy. The estimated eigenfrequencies from network are compared to the target values in Figure 17.

For the application of the hybrid neuro-genetic technique, the genetic algorithm part is set-up: population size, $N = 150$; crossover-rate, $C = 0{\cdot}35$; and mutation rate, $M = 0{\cdot}02$. Each parameter is represented as a 29-bit binary number, roulette wheel selection method is adopted for the selection.

Two different cases are considered. (a) A crack of depth α of 0·0048 m exists at L_1 of 1·5125 m. The first three eigenfrequencies are obtained computationally; $f_1^* = 266{\cdot}73$ rad/s, $f_2^* = 1149{\cdot}32$ rad/s, $f_3^* = 1788{\cdot}86$ rad/s. (b) A crack of depth α of 0·0033 m exists at L_1 of 2·8875 m. The first three eigenfrequencies are obtained computationally; $f_1^* = 266{\cdot}94$ rad/s, $f_2^* = 1151{\cdot}63$ rad/s, $f_3^* = 1845{\cdot}38$ rad/s. Figures 18 and 19 illustrate convergence history of the fitness functions for case (a) and case (b) respectively.

The searches meet the convergence after 38 and 29 iterations for case (a) and case (b) respectively. Table 2 shows the location and depth of a crack as estimated by the hybrid neuro-genetic technique with 6·5% error. Also, the corresponding eigenfrequencies are very close to the reference values within 0·18% error.

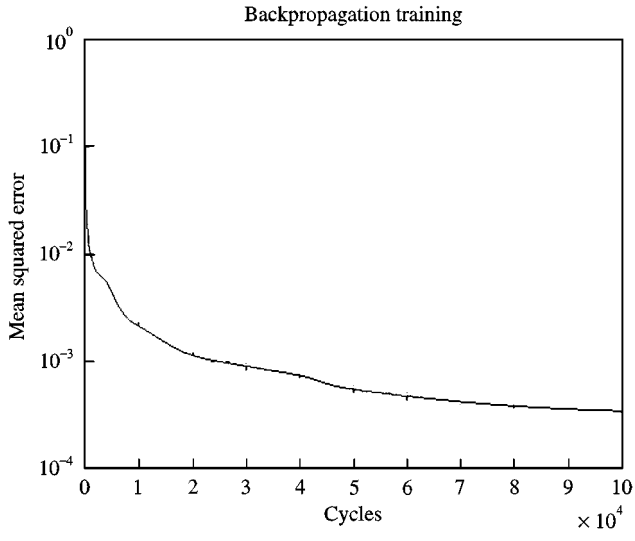

Figure 16. Neural network training output.

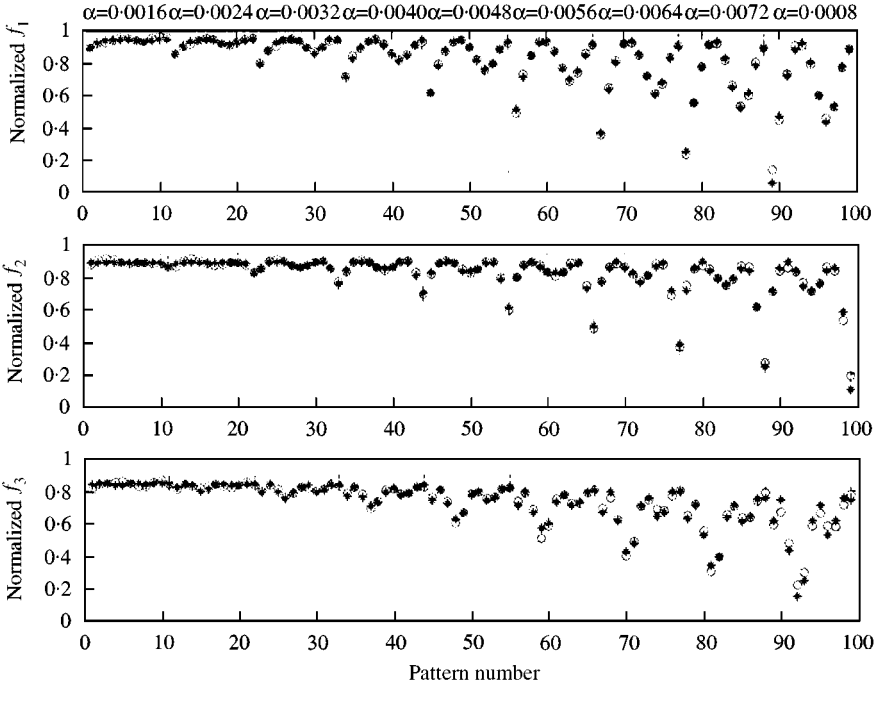

Figure 17. Comparison of the estimated eigenfrequencies from neural network to target values. ∗ target value; ○ estimated value.

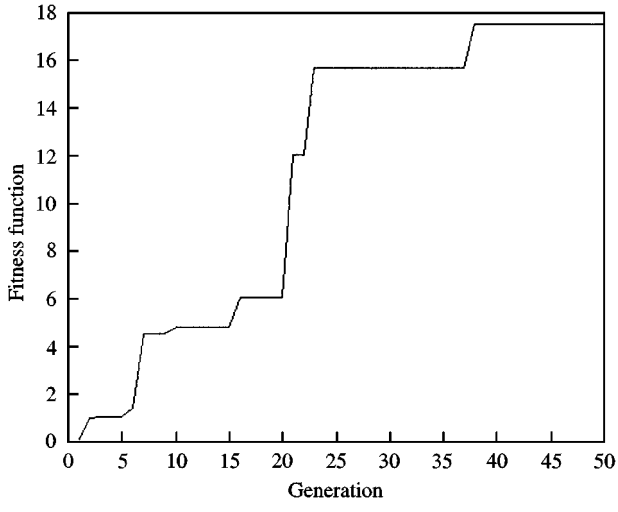

Figure 18. Generation history of Case (a).

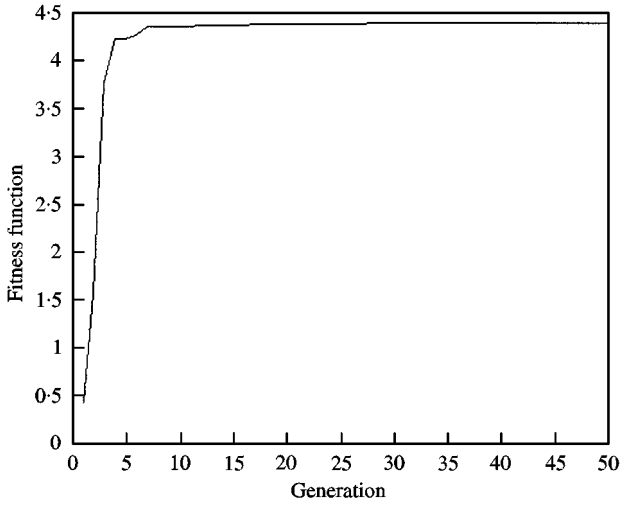

Figure 19. Generation history of Case (b).

TABLE 2

Crack identification result: clamped–clamped plane frame

	Case (a)			Case (b)		
	Reference value	Result value	Relative error (%)	Reference value	Result value	Relative error (%)
a (m)	0·0048	0·0051	6·25	0·0032	0·0033	3·12
L_1 (m)	1·5125	1·5512	2·56	2·8875	2·8856	− 0·06
f_1 (rad/s)	266·73	266·55	− 0·06	266·94	266·47	− 0·18
f_2 (rad/s)	1149·32	1149·18	− 0·01	1151·63	1151·62	− 0·001
f_3 (rad/s)	1788·86	1788·92	0·003	1845·38	1845·42	0·002

6. CONCLUSIONS

A methodology of hybrid neuro-genetic technique for the crack identification from the eigenfrequencies is proposed based on the fact that a crack has an important effect on the dynamic behavior of a structure. To estimate the crack parameters neural network and genetic algorithm are combined into the proposed technique. The neural network is for the approximation of the eigenfrequencies as the functions of the crack parameters and the genetic algorithms is for finding crack parameters which minimize the difference from the measured eigenfrequencies.

The effectiveness of this technique is confirmed by two example problems. The crack parameters of the clamped–free beam problem are estimated within 5% error. In the case of the clamped–clamped plane frame problem the estimation has shown agreement within 6·5% error. It can be concluded that good agreements are obtained between the estimated crack depth and location and the reference ones.

The hybrid neuro-genetic technique can be generalized for general boundary condition and structure to estimate the crack location and depth provided that the reference data, or training data to train the neural network are properly prepared.

ACKNOWLEDGMENTS

The authors are grateful for the support provided by a grant from the Korea Science & Engineering Foundation (KOSEF) and Safety and Structural Integrity Research Center at the Sungkyunkwan University.

REFERENCES

1. T. C. CHONDROS and A. D. DIMAROGONAS 1979 *ASME Design Engineering Technical Conference, St. Louis.* Identification of cracks in circular plates welded at the contour.
2. T. C. CHONDROS and A. D. DIMAROGONAS 1980 *Journal of Sound and Vibration* **69**, 531–538. Identification of cracks in welded joints of complex structures.
3. G. D. GOUNARIS and A. D. DIMAROGONAS 1988 *Computational Structure* **28**, 309–313. A finite element of a cracked prismatic beam in structural analysis.
4. G. D. GOUNARIS and V. PAPAZOGLOU 1992 *Computational Structure* **42**, 769–779. Three-dimensional effects on the natural vibration of cracked Timoshenko beams in water.
5. T. INAGAKI, H. KANKI and K. SHIRAKI 1981 *Journal of Mechanical Design* **104**, 1–11. Transverse vibrations of a general cracked rotor bearing system.
6. P. S. LEUNG 1992 *Rotordynamics* '92, *International Conference on Rotating Machine Dynamics, Venice.* The effects of a transverse crack on the dynamics of a circular shaft.
7. N. ANIFANTIS, P. RIZOS and A. D. DIMAROGONAS 1987 *Proceedings of the* 11*th Biennial ASME Conference on Mechanical Vibration and Noise, Boston.* Identification of cracks on beams by vibration analysis.
8. A. D. DIMAROGONAS and G. MASSOUROS 1981 *Engineering Frature Mechanics* **15**, 439–444. Torsional vibrations of a shaft with a circumferential crack.
9. H. G. NIKOLAKOPOULOS, D. E. KATSAREAS and C. A. PAPADOPOULOS 1997 *Computer & Structures* **64**, 389–406. Crack identification in frame structures.
10. T. FURUKAWA and G. YAGAWA 1995 *International Conference on Computational Engineering Science Computational Mechanics* '95 Springer-Verlag, 122–127. Parameter identification using an evolutionary algorithm and its performance under measurement errors.
11. S. KUBO 1993 *Inverse Problem.* Baifu-kan (in Japanese).
12. Q. SHI and I. HAGIWARA 1999 *Proceedings of the ASME Design Conference on Engineering Technology.* Structural damage detection and identification using learning vector quantization neural network.

13. P. TSOU and M. H. SHEN 1993 *AIAA-93-1708-CP*, 3551-3560. Structural damage detection and identification using neural network.
14. I. HAGIWARA, Q. SHI and A. INOUE 1997 *Proceedings of the International Symposium on Optimization and Innovative Design* 97, *Tokyo*, *Japan* (*in CD-ROM*) *JSME*. Development of inverse analysis methods applicable to modification calculation model by using experimental data.
15. W. D. PILKEY and W. WUNDERLICH 1994 *Mechanics of Structures Variational and Computational Methods*. Boca Raton: CRC Press.
16. C. A. PAPADOPOULOS and A. D. DIMAROGONAS 1988 *Journal of Vibrational Acoustics Stress and Reliability Design* **110**, 1–8. Coupled longitudinal and bending vibrations of a cracked shaft.
17. H. TADA 1973 *The Stress Analysis of Cracks Handbook*. PA: Del Research Corporation.
18. P. TSOU and M. H. SHEN 1994 *American Institute of Aeronautics and Astronautics* **32**, 176–183. Structural damage detection and identification using neural network.
19. D. E. RUMELHART, G. E. HINTON and R. J. WILLIAMS 1986 *Parallel Distributed Processing*: *Exploration in the Microstructure of Cognition* **1**, 318–362. Learning internal representations by error propagation.
20. M. GEN and R. CHENG 1997 *Genetic Algorithms and Engineering Design*. New York: Wiley-Interscience Publication.